Journal of Environmental Management 373 (2025) 123573

Contents lists available at ScienceDirect

Journal of Environmental Management

journal homepage: www.elsevier.com/locate/jenvman

Research article

Tracing the trail of eroded fertile soils during a high intensity rainfall event: A fingerprinting study in war-torn tropical mountains

Ivan Lizaga[a,*], Montfort Bagalwa[b,c], Borja Latorre[d], Kristof Van Oost[b], Ana Navas[d], William Blake[e], Pascal Boeckx[a]

[a] Isotope Bioscience Laboratory - ISOFYS, Department of Green Chemistry and Technology, Ghent University, Coupure Links 653, 9000, Gent, Belgium
[b] Earth and Life Institute, Université Catholique de Louvain, Louvain-la-Neuve, Belgium
[c] Service Environnement, Observatoire Volcanologique de Goma (OVG), Goma, Democratic Republic of the Congo
[d] Estación Experimental de Aula-Dei (EEAD-CSIC), Spanish National Research Council, Zaragoza, Spain, Avenida Montañana, 1005, 50059 Zaragoza, Spain
[e] School of Geography, Earth and Environmental Sciences, University of Plymouth, UK

A R T I C L E   I N F O

Handling editor: Lixiao Zhang

Keywords:
Soil degradation
Sediment fingerprinting
Extreme storm events
Banana plantations
Water quality decrease

A B S T R A C T

The depletion of fertile topsoil presents a critical challenge in tropical mountain agroecosystems. Impacts are intensified during heavy storm events that strip unprotected topsoils and pose risks to downstream water ecosystems. To better understand such dynamics, we investigated an agricultural mountainous catchment located on the Democratic Republic of the Congo shore of Lake Kivu. This area is characterised by weak governance systems exacerbated by protracted violent conflicts, which have prevented the application of remediation practices to address extensive land use changes, including deforestation and monoculture proliferation, notably banana plantations. Additionally, the spread of Banana Xanthomonas wilt (BXW) has further augmented land use impacts. Herein the complete diseased mat uprooting (CDMU) method employed to combat the disease has resulted in significant erosion and sediment export rates. Following the recovery of banana plantations from CDMU, sediment export rates continued to increase without a clear responsible party but more as a legacy of past and present land degradation activities and embedded soil erosion and connectivity process pathways.

To analyse the impact of high-intensity storm events coupled with the aftermath of conflict instability and the effects of BXW on erosion dynamics, the sediment fingerprinting technique was implemented. We collected 60 sediment source samples across a 42 km^2 catchment, predominantly cultivated since the mid-20th century. Samples spanned four main land uses/land covers: seasonal crops, banana plantations, bare or degraded soil, and channel banks. Additionally, mixture/target samples were collected at the summit of six fluvial terraces located at different altitudes along the vertical profile of the river after a high-intensity storm event. These terraces serve as natural indicators of sediment accumulation under different flow intensities, with higher terraces representing sediment deposition during higher discharge. Furthermore, sediment samples were collected via a gravity core in delta deposits at the river's inflow into the lake, allowing us to identify the main sources contributing to fine sediment export to the lake. This methodology enabled us to assess how sediment provenance has changed in response to varying discharge levels while elucidating the primary sources responsible for fine sediment inputs to the lake and the subsequent water quality decrease.

Our analysis indicates increased contributions occurred from channel banks and degraded areas as discharge increased. Despite steep channel banks and degraded soils being primary sediment sources on the terraces, agricultural and banana sources predominantly contributed to the fine sediments exported to the lake. These findings underscore the hazards of high-intensity storm events in these fragile ecosystems and highlight the role of current banana plantation and cropland management in degrading land and water quality.

Understanding the primary factors driving land degradation and sediment export is crucial for preventing further ecosystem degradation and mitigating heightened instability in conflict-affected areas. This research suggests that remediation practices should be incentivised to create buffer structures in upslope agricultural areas and protect the fertile sediments from banana plantations from being exported to the lake if socio-cultural and economic hurdles to implementation can be overcome.

* Corresponding author.
E-mail addresses: ivan.lizaga@ugent.be, lizaga.ivan10@gmail.com (I. Lizaga).

https://doi.org/10.1016/j.jenvman.2024.123573
Received 1 August 2024; Received in revised form 18 November 2024; Accepted 1 December 2024
Available online 9 December 2024

1. Introduction

The impact of soil erosion on tropical mountain agroecosystems has received increasing attention due to the vulnerability of shallow and unprotected soil to erosion processes, which are the main cause of soil loss and subsequent land degradation. In tropical environments, particularly those vulnerable to intense rainstorms after dry periods, exceptional rain events have been identified as major contributors to geomorphological changes, including piping, gully formation, landslides, and subsequent soil loss (Depicker et al., 2021; Lutete Landu et al., 2023; Vanmaercke et al., 2016). The significance of these high-intensity rainstorms and the resulting runoff lies in their ability to rapidly accelerate soil and bedrock erosion on hillslopes, often leading to increased sediment mobilization and changes in sediment sources released into streams (Navas et al., 2004; Winston and Criss, 2002). Storm intensity plays a crucial role in these processes, as intense rainstorms can contribute significantly to geomorphological changes and soil loss (Baumgartner et al., 2022). However, little is known about the effect of different rainfall intensities on the provenance of the exported sediment, a growing concern with climate change.

The export of fine sediment bears significant off-site consequences, notably the rapid siltation of downstream water bodies, reaching peak impact in areas affected by sudden human disturbances, such as violent conflicts and subsequent internal population displacement that can result in deforestation, soil degradation, and overexploitation of natural resources (Maystadt et al., 2020). This is especially marked in tropical landscapes, like the African Great Lakes region, which has experienced sudden changes in sediment export due to the prevalence of conflict instability that disrupts traditional land management practices, interrupts agricultural activities, and hinders conservation efforts. Furthermore, the proliferation of monocultures, notably banana plantations, further intensifies the vulnerability of these landscapes to erosion processes. Specifically, the spread of Banana Xanthomonas wilt (BXW) has exacerbated these challenges by causing sudden land clearing in affected regions. Remediation practices, such as the Complete Diseased Mat Uprooting (CDMU) method, have been widely implemented to combat the disease. This method involves uprooting infected banana mats and burying them in the soil, leaving the soil disturbed and unprotected, often with a transition to seasonal crops and increased erosion rates (Ocimati et al., 2020). Therefore, to effectively control soil erosion, it is crucial to identify the most susceptible areas, soils, or land use exposed to erosion processes and the specific cause leading to soil loss in these complex landscapes. For these reasons, defining the sources of eroded fine-grained sediment is a vital requirement for catchment management, as well as for understanding the evolution of landscapes and delineate the most sensitive areas to lose soil.

Determining sediment provenance in catchments where access is limited using conventional monitoring techniques is often challenging, but in most environments, it can be undertaken by applying sediment source fingerprinting methods (Owens et al., 2016). To date, there are several studies on identifying source apportions by fingerprinting techniques (Blake et al., 2012; Clarke, 2014; Evrard et al., 2013; Gruszowski et al., 2003; Palazón et al., 2015; Walling, 2005) but only few have quantified the sediment provenance after an exceptional rainstorm event (Gaspar et al., 2019; Lizaga et al., 2019; Martínez-Carreras et al., 2010; Zhang et al., 2017). Notably, none have comprehensively analysed changes in source contributions during such events and traced their transport to downstream water bodies, such as lakes.

Our study addressed this gap by investigating sediment provenance at various altitudinal levels along a vertical profile of fluvial terraces. These terraces, positioned at different altitudes, offer a unique opportunity to analyse sediment deposition under varying flow intensities in a single storm event. By collecting sediments accumulated at the top of each terrace after a high-intensity storm event, we aimed to replicate sediment deposition patterns corresponding to different discharge levels; higher terraces requiring greater discharge to reach. Additionally, we analysed sediment cores at the river's inflow to the lake to determine the sources contributing fine sediments to the lake. This approach provides valuable insights into sediment transport dynamics in highly degraded tropical landscapes.

Our objectives were threefold: (i) to analyse variations in sediment properties across different flow discharges during a high-intensity rainstorm event in a tropical mountain agroecosystem; (ii) to quantify and track changes in sediment provenance corresponding to variations in flow intensity, with a focus on the Lake Kivu region, which has experienced rapid land-use changes and intensified erosion processes due to factors such as conflict, population displacement, and the spread of banana diseases; and (iii) to identify the primary contributors of sediments reaching the lake. Thus, our multi-faceted approach, integrating spatiotemporal analysis of soil properties with the state-of-the-art fingerprinting modelling, aimed to elucidate how high-intensity storm events alter streambed sediments and the shifts in sediment contributions from various sources. Our study presents a unique opportunity to observe the impact of storm events on sediment contribution, facilitated by the availability of terraced sediments and lake sediment cores post-storm event.

2. Material and methods

2.1. The study area

The study area is situated in the northwestern part of the Lake Kivu region, positioned within the highest segment of the Albertine Rift in Central–East Africa, covering an area of approximately 180,000 km^2 (Fig. 1). The terrain exhibits a steep elevation profile, with lowlands ranging between 1000 and 1500 m a.s.l and highlands reaching heights of 2000–3500 m a.s.l, encompassing the Congo–Nile ridge and the volcanic chains of Virunga (Nahimana, 2015).

Our investigation focused on a medium-sized catchment spanning 42 km^2, drained by the Renga River, as representative of the severe deforestation and land use change in the region. The altitudinal profile of the study area extends over 8.6 km, from the lowest point at the Renga River outlet (1460 m a.s.l) to the upper region exceeding 2800 m a.s.l. Climatically, the lowlands receive annual precipitation ranging between 1000 and 1200 mm, while the highlands experience higher precipitation levels of 1300–1550 mm per year, accompanied by an average annual temperature of 19 °C (Ndayirukiye and Sabushimike, 2015). The precipitation pattern is primarily bimodal, featuring a major dry season from June to August, a primary wet season from February to June, a minor dry season from January to February, and a major wet season from September to December (Bagalwa et al., 2021). Geologically, the lithology of the Renga catchment is characterised by basic volcanic formations such as basalts, ash, tuff, and lavas. Pedologically, the area features Acrisols and young fertile Andosols on volcanic terrains with a sandy-loamy texture (Dewitte et al., 2013; Nahimana, 2015).

The vegetation cover presents a mosaic of various seasonal crops that dominate the highlands together, with banana plantations predominating in the lower valley regions. Pristine forest cover is scarce or inexistent due to decades of agricultural expansion, with newly formed forests in abandoned agricultural areas and grasslands or herbaceous vegetation primarily composed of recently abandoned crops or under rotation barely occupying 30% of the area. Agriculture covers more than 50% of the Renga catchment, with banana plantations constituting 30% of the total and dominating the lowlands (Buchhorn et al., 2020; Zanaga et al., 2022). The agricultural landscape mainly comprises seasonal crops such as cassava, maize, and beans alongside perennial crops, primarily bananas.

2.2. Soil sampling and analysis

During fieldwork campaigns, potential sediment sources and sediment sampling locations were identified with particular attention to landscape evolution over the last decades, as well as changes in the main channel and the progradation of the delta located downstream.

A total of 66 source sediment samples were collected using a trowel, collecting the top 2 cm with four replicates at each sampling point. These replicates were combined in the field to create a representative composite sample. Samples were obtained from different land uses, including croplands (AG), banana plantations (BAN), degraded areas (DEG), and channel banks (CB). Source samples were distributed across the catchment and along the main streams, ensuring connectivity and representation of the percentage of each land use area. Samples from recent degraded areas (DEG) were collected at landslide scars, both those formed during the studied high-intensity rainfall event as well as pre-existing landslides, near stone extraction activities, or mounds of sediments extracted from the stream channel beds and dumped close to the main channels (Fig. 1f). Additionally, channel bank samples were collected along the main streams.

According to rainfall data from the GPM satellite product, the catchment experienced an accumulated precipitation event between November 29–30, 2022, totalling 69.9 mm (Huffman et al., 2019). This amount of rainfall is typical of events associated with landslides and flash floods in the region (Monsieurs et al., 2018). For this study, six sediment mixture samples were collected after this high-intensity rainfall event in the upper part of a vertical profile of fluvial terraces in the active riverbed near the catchment outlet to trace deposited fine sediment changes with variations in water discharge during a single high-intensity storm event (Fig. 1e–f). Consequently, higher discharge led to fine sediment deposition on higher terraces (i.e., higher altitude from the active channel), whereas low discharge led to sediment deposition on terraces at lower altitudes. This type of sampling allows us to understand not only the sediment contribution to the stream but also how it varies with the intensity of discharge changes produced during a high-intensity storm event.

Additionally, to understand the export dynamics, we collected two gravity cores at the inflow of the river into the lake to track the sediment exported from the hillslopes to the lake during the event. Due to the high sediment loads, the cores were collected 50 m and 100 m away from the river inflow to prevent clogging of the UWITECH gravity core sampler (UWITECH, Austria) by branches, debris, and leaves. However, due to the high organic material and debris content exported, the depth of the cores was limited, and subsequently, the quantity of sediment.

Magnetic susceptibility (MS) was measured contiguously at 2 mm intervals along the length of the core halves, using a Bartington MS2E point sensor with spatial resolution of 3.8 mm mounted on a Geotek Multi-Sensor Core Logger (MSCL) to delineate possible storm events in the collected sediment cores.

The samples were air-dried, ground, homogenised, and sieved to ≤0.150 mm. It was decided the use of ≤0.150 mm due to the predominant sandy-silt fraction of the sediment mixtures and due to the high discharge events, which mobilise higher particle size than the standard 0.063 mm employed in most sediment fingerprinting studies. In addition, to minimize the potential particle selection effect for the fluvial terrace samples, we collected only the top layer containing the finest sediments, which likely represents the suspended sediment deposited during the storm event (Fig. 1e).

Following the same methodologies as in Lizaga et al. (2019) particle size and stable elements were analysed. A Beckman Coulter LS 13320 laser diffraction particle size analyzer was used for grain size analysis. Prior to particle size measurements, the organic fraction was removed

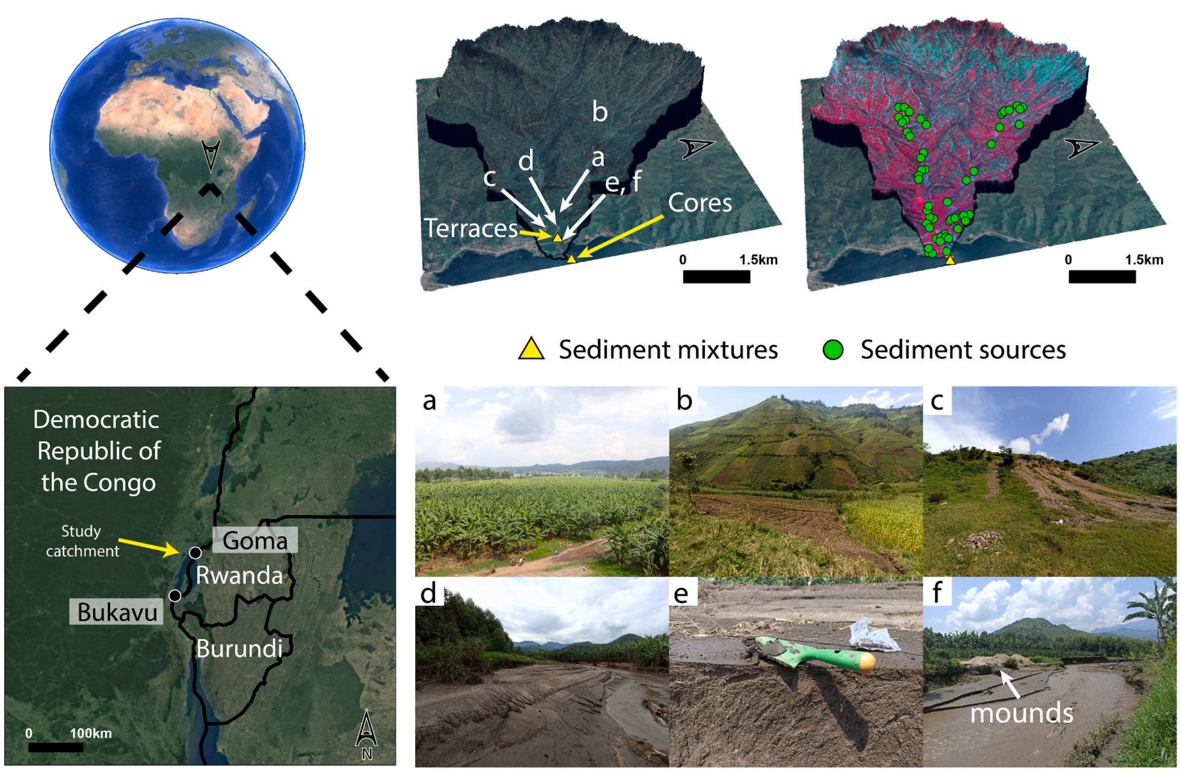

Fig. 1. Location of the study area (−1.675688°, 28.988907°) and 3D representation of Renga catchment. Left: RGB representation; Right: False-colour composition (SuperDove Planet satellite imagery from December 2022, NIRGB band combination) with red colours indicating higher vegetation density and cyan colours representing crops or surfaces with no vegetation cover. (a–f) Photographs taken on December 5, 2022, illustrating various land use/land cover areas targeted as potential sources: (a) Banana plantation; (b) highlands crops characterised by steep slopes and rilling processes; (c) degraded areas used for rock extraction; (d) floodplain displaying clear signs of runoff erosion with steep channel banks at the bottom of the picture. (e) fine sediment mixture sample collection in one of the terraces. (f) cross-sectional image of the Renga River, revealing different terraces left after the storm event and mounds of dredged bedchannel sediments extracted from the river, also considered part of the degraded areas due to the similar characteristics. These sediment piles, locally extracted from the riverbed and accumulated for removal or levee construction, have been regarded as a sediment source due to their proximity to the channel.

by H_2O_2 (10%) heated to 80 °C. Samples were then chemically dispersed with 2 ml of sodium hexametaphosphate (40%), stirred for 2 h and sonicated for a few minutes to facilitate dispersion. Stable element analyses were performed using X-Ray Fluorescence (XRF) with a Niton XL3T 950 He GOLDD + XRF Analyzer. Major and minor elements (Si, Al, Fe, Ca, K, Zr, Sr, U, Rb, Th, Pb, As, Zn, Cu, Ni, Mn, Cr, V, Ti, Sc, Ba, Nb, Bi, P, Cl) were measured, and concentrations, obtained after three measurements per element, are expressed in ppm.

2.3. Tracer selection methods and unmixing model

An essential criterion for tracer selection methods is to exclude non-conservative tracers from being incorporated into the models, as their inclusion may lead to erroneous outcomes (Collins et al., 2017; Haddadchi et al., 2013; Owens et al., 2016; Smith and Blake, 2014). Some tracers fall outside the range of sediment source values due to their lack of conservativeness, sediment particle size effects or external factors such as contamination. Tracer selection is crucial for a successful unmixing and negatively affects all types of models, either Frequentist or Bayesian (Pulley et al., 2015; Cooper and Krueger, 2017; Lizaga et al., 2020a; Latorre et al., 2021).

In order to extract all the possible information of our tracers, we implemented state-of-the-art methods, such as the Conservativeness Index (CI), Consensus Ranking (CR) and the Consistent Tracer Selection (CTS) to i) extract the source apportionment predictions that each tracer introduces into the model and identify non-conservative tracers based on that information and ii) unravel the presence of multiple consistent solutions present in over-determined datasets (more or equal number of tracers than sources). CI is a non-parametric test that analyses tracer conservativeness using mixture and source data to create an index as a more sophisticated version of the range test. CR is a scoring function based on several random debates between tracers, in which the tracers preventing consensus are assigned low scores (Lizaga et al., 2020a). Consensus-reaching processes proceed in a convergent multistage way, where experts present their opinions and discuss and negotiate to bring positions closer by modifying their initial opinions (Pérez et al., 2018). In fingerprinting studies, the mentioned experts are the tracers in the dataset. CTS, similar to the discriminant function analysis (DFA), identifies the most discriminant tracers, but it also examines their mathematical properties to ensure consistency in over-determined datasets (Latorre et al., 2021).

Based on the mathematical nature of the unmixing models, for four sources, a minimum of $n – 1$ tracers are required (n being the number of sources) to obtain a determined system of equations with one possible solution. Thus, a minimum of three tracers are required to unmix four sources. To implement the tracer selection for unmixing, the methods mentioned above were used to remove those tracers with apparently non-conservative or non-consensual behaviour and select an optimal set of tracers for each mixture. The most discriminant triplet of tracers with a conservative solution extracted from the CTS analysis was extended, incorporating additional consistent tracers from the dataset with a maximum error threshold $\varepsilon = 0.025$. To estimate the relative contribution of each potential sediment source to the mixtures, a validated Frequentist fingerprinting model implemented as an R package-FingerPro v2 (Lizaga et al., 2018, 2020b) was applied.

3. Results

3.1. Major elements concentration and sediment source discrimination

The measured properties of the sediment mixtures collected in the fluvial terraces and the sediment cores are shown in Fig. 2, and their correlation in Fig. S1. Mean contents of silt and clay fractions decreased from 70.06% and 11.94%, respectively, in the sediment collected in the cores to 40.17% and 6.48% in the fluvial terraces, while the sand fraction increased from 18.00% in the cores to 53.35% in the terraces (Fig. 2 & Table S1).

For this reason, the element content that positively correlated with the fine fraction, such as Zr, Sr, Pb, As, Zn, Cu, Fe, Cr, V, Ti, Ba, Nb, Al, P, and Cl, had a lower concentration in the fluvial terraces than in the core sediments. On the contrary, the elements that positively correlated with the coarse fraction, such as Th, Ca, and Bi, were enriched in the sediment collected on the fluvial terraces.

The statistics of the trace element properties for the potential sediment sources are presented in Table 1. As expected, both CB and DEG sources presented higher concentration of sand-size particles, with mean values of 66% and 50%, while AG and BAN sources had 32% and 30%, respectively.

Tracers offered notable source discrimination (Fig. 3) when all tracers were used together with no apparent overlap between the four potential sources. As expected, degraded areas (DEG) and channel banks (CB) displayed the most notable discrimination, while seasonal crops (AG) and banana plantations (BAN) showed closer similarities.

3.2. Sediment source contributions under different discharge

The unmixing model results from the fluvial terraces samples revealed a dominant contribution from channel bank (CB) sources, ranging from 17.1% to 59.2% (Fig. 4). Given that the different terraces sampled represent varying discharge regimes, a change in source contribution with increasing discharge can be inferred. Starting from T5, representing higher discharge intensity, the contribution of geomorphological features dominated (i.e. CB and DEG), despite the proximity of the banana plantation source. T4, also representing high discharge, displayed similar pattern with higher contribution of CB and a reduction of BAN in favour of the AG source. For lower terraces and discharge intensities, T3 located on the right margin of the river yielded similar results but with DEG predominating due to river morphology and proximity of the DEG source in the form of mounds of channel-bed sediments extracted from the stream bed by farmers and accumulated on stream levees after storm events. Transitioning to T2 and T1, we observed a shift from geomorphological features to AG and BAN dominance, suggesting the export of finer sediments and stability of talus at medium discharge intensities. Finally, at low discharge intensities (T0), CB predominated again.

BAN, although generally the least contributing source, showed significant contributions alongside AG in medium-low discharge intensities at T1 and T2. Contrary to this pattern, we see a high BAN contribution in T5, likely linked to the proximity of banana plantations experiencing high runoff.

3.3. Sediment source exports to Lake Kivu

In our analysis of sediment source exports to Lake Kivu, we observed that while a significant portion of sediments deposited in the terraces and the river channel bed originated from CB and DEG (approx. 55%), the sediment reaching the lake is predominantly sourced from BAN and AG sources. An assessment of the two short cores analysed in this study (Figs. 5 and 6) revealed that, overall, 50%–80% of the recent sediment deposited in the submerged delta can be attributed to agricultural land, including both croplands and banana plantation sediments. In addition, in the finer fraction deposits, the contribution of BAN/AG is mostly higher than 60%, with a predominance of BAN contribution. These results align with the predominance of steep slope agriculture upstream and the predominance of banana plantations surrounding the streams. As can be seen in Table S1, AG and BAN have higher content of fine particles, which makes them more easily transported downstream, being predominant as the source of contribution to the lake with a lower residence time in the streams.

The magnetic susceptibility and grain size data measured in the cores suggest that C1 represents deposition from a single storm event while C2 likely represents two different storm events of different intensities. The

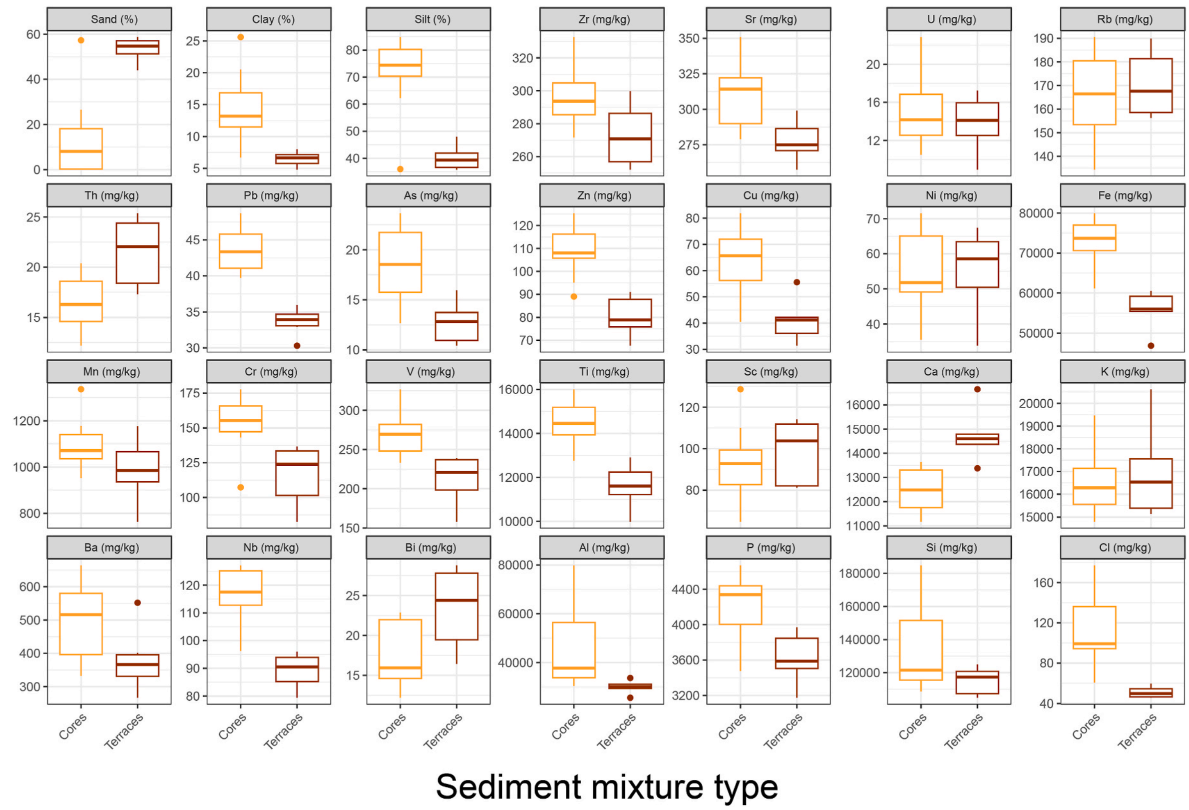

Fig. 2. Boxplot of the sediment properties from the sediment cores (yellow) and fluvial terraces (brown) samples.

Table 1
Mean, median and standard deviation values of the trace elements for the potential sources — croplands (AG), banana plantations (BAN), degraded areas (DEG), and channel banks (CB).

Tracer	AG			CB			BAN			DEG		
	mn	md	sd	mn	md	sd	mn	md	sd	mn	md	sd
Zr (mg/kg)	263.5	260.9	48.7	247.4	243.7	41.5	266.5	266.9	44.4	302.4	246.5	83.1
Sr (mg/kg)	394.8	377.1	135.3	363.2	373.2	47	477.7	325.9	383.7	256.2	302.8	92.5
U (mg/kg)	15.8	12	10.3	20.2	19	13.2	18	18.4	6.7	11.5	11.5	1.4
Rb (mg/kg)	121	110.4	43.5	121.6	122.4	16.6	161.3	152.6	50	140.2	146.7	26.2
Th (mg/kg)	16.2	14.2	8	12.4	12.1	2.4	28	24.5	15.1	15	15.1	4.3
Pb (mg/kg)	35.1	35.2	6.3	36.2	36.3	4.7	32.3	32.3	4.5	25.9	25.3	5.8
As (mg/kg)	10.4	8.9	4.9	10.5	11.3	1.9	11.3	12.5	2.3	37.8	36	26.8
Zn (mg/kg)	86.1	85.4	19.8	134.4	129.5	33.9	91.4	95.8	12.8	71.9	67.7	40.3
Cu (mg/kg)	64.8	63.5	15.6	63.2	70.4	13.1	51.1	44.5	23	49.3	49.2	6.7
Ni (mg/kg)	78.6	78.2	23.2	103.8	100.5	40.4	91.8	91.8	14.7	41.3	41.4	2.5
Fe (mg/kg)	71,860	72,110.7	10,511.1	72,948.3	72,957.7	4170	63,392.6	65,864.1	13,509.1	53,224.4	48,665.2	24,948.8
Mn (mg/kg)	1539.7	1547	378.4	1547.6	1615.5	135.2	1148.6	1341.5	358.4	858.5	1005	390
Cr (mg/kg)	148.9	142.9	38.3	137.3	137.9	27	148.8	126.6	52.6	163.6	155.7	54.9
V (mg/kg)	280	294.7	55.1	248.8	240.5	30	213.4	213.3	51.1	236.3	236.9	2.9
Ti (mg/kg)	14,406.6	14,232.7	3126.1	13,663	14,009.8	2406.6	12,404.3	12,839.7	2345.6	12,118	10,771.4	3595.6
Sc (mg/kg)	149.3	134.6	61.6	192.1	193.3	71.7	162.1	150.7	79.3	141.9	142	9.1
Ca (mg/kg)	20,278.8	19,990.4	6903.3	24,317.9	22,153.5	10,789.1	27,751.8	21,341.2	17,712.1	16,145.6	16,300.3	9437.9
K (mg/kg)	11,298.4	11,303.4	3171.7	14,174.4	14,558.6	2174.4	19,019.9	19,029.9	4297	21,433.8	17,659.7	10,513.7
Ba (mg/kg)	562.7	535	161	496.1	487.7	151.6	472	441	113	666.5	661.5	265.1
Bal (mg/kg)	727,886.9	731,291.3	17,598.6	710,179.5	711,771.6	13,720.9	702,939.9	710,217.7	24,651.5	713,075.2	729,961.5	37,950.5
Nb (mg/kg)	113.2	114.8	25.5	102.8	99.3	16.3	98.5	100.1	23.5	74	75.5	24.6
Bi (mg/kg)	17	13.5	10.1	12.6	12.3	3.2	31.6	27.1	20.1	33.3	18.9	27.4
Al (mg/kg)	27,686.9	27,975.8	5085.4	25,719.9	25,914.4	2981.2	31,525.2	33,922.7	4597.6	34,435.6	36,890.6	7476.7
P (mg/kg)	4478.8	4700	1068.2	5680.1	5777.4	1035.6	4609.3	4586.3	947.8	2873.8	2693.3	1387.8
Si (mg/kg)	116,206.9	115,311.2	20,711.8	128,136	130,138.6	4823.6	131,520.1	136,269.4	14,238.1	142,074.9	144,731.3	7737.3

different stages of the storm event can be distinguished in Figs. 5 and 6 with grain size being coarser during the peak of the rainfall event and finer at the beginning and the end when the flow energy is low. Thus, in C1, this hysteresis cycle is characterised by fine sediments at the bottom, representing the initial stages of stormflow, a layer of coarse sediments representing the maximum discharge intensity that gradually reduces towards the top while increasing in the silt and clay fraction, likely representing a lower transport capacity and discharge.

The sediment source contribution exhibits a similar pattern. At the bottom, the sediment contribution is dominated by AG and BAN sources.

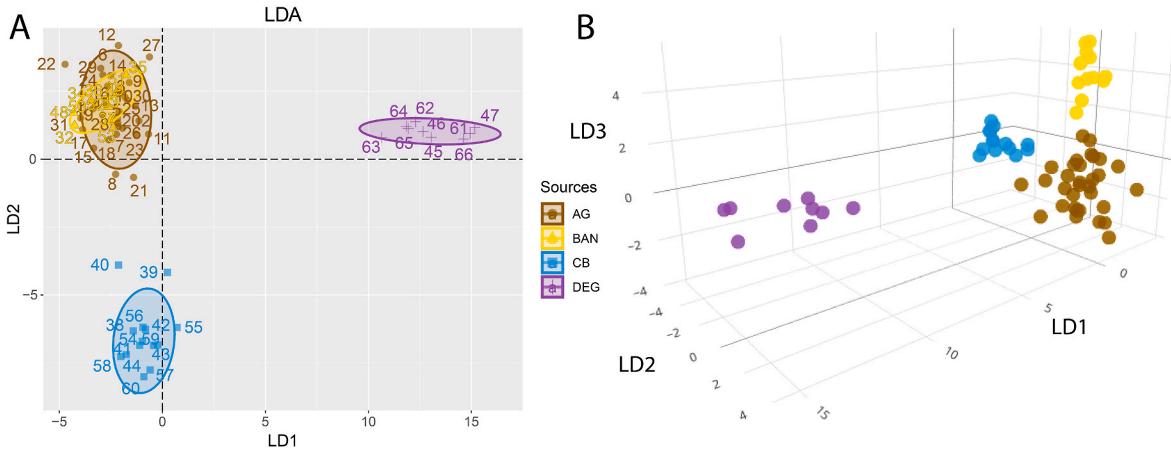

Fig. 3. Linear discrimination analysis (LDA) graph of the sediment sources (agricultural – AG, banana plantation – BAN, channel bank - CB, degraded areas -DEG) for the elemental tracers. A) 2D LDA and B) 3D LDA.

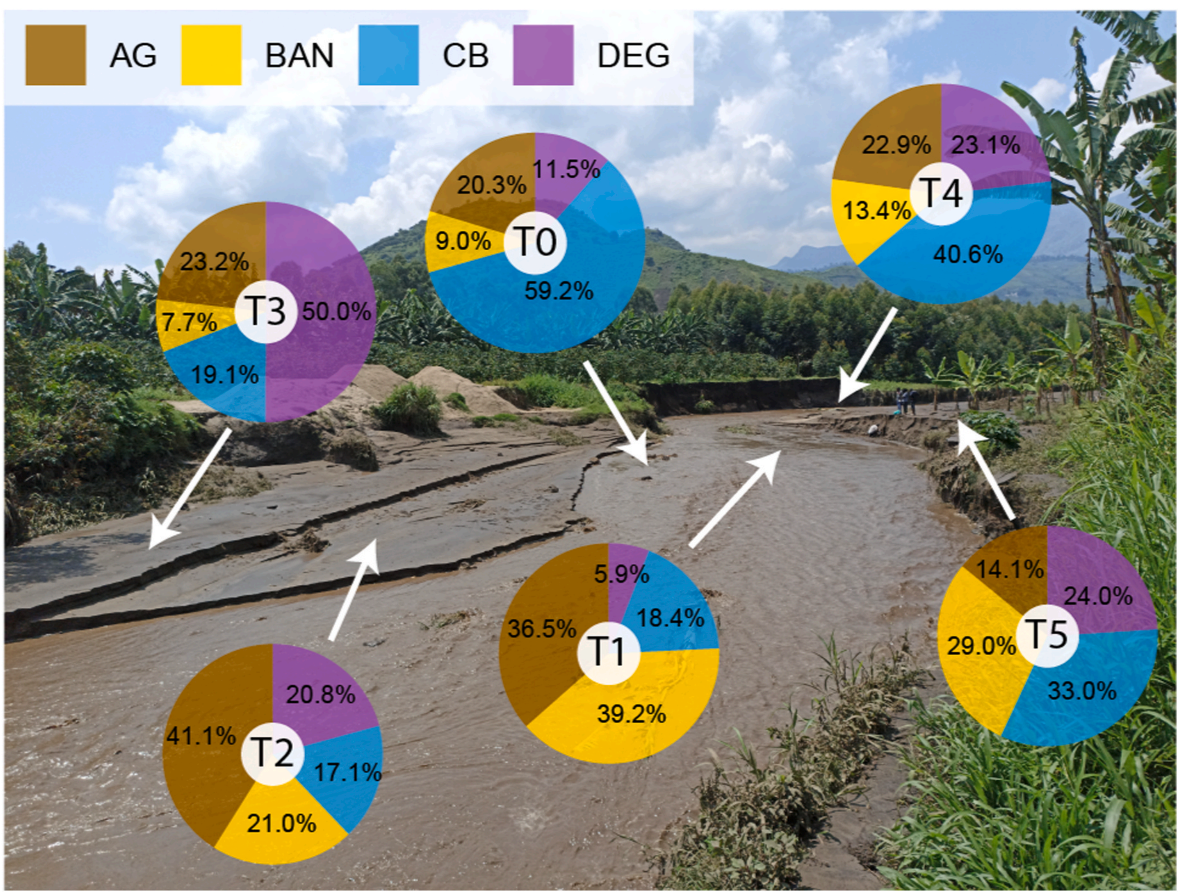

Fig. 4. Pie chart of the proportional contribution from each sediment source to the sediment mixtures collected after a high-intensity rainfall event in the upper part of a vertical profile of fluvial terraces (T0 – T5). Consequently, higher discharge led to fine sediment deposition on higher terraces (i.e. T5 max flow), whereas low discharge led to sediment deposition on terraces at lower altitudes (i.e. T0 base flow).

During the high discharge intensity represented by coarser sediments, the sediments predominantly originate from geomorphic features (CB and DEG). However, this contribution from geomorphic features gradually reduces towards the top, being replaced by a predominance of AG and BAN sources. This is supported by the gradual decrease of the magnetic susceptibility values and the decrease in the contribution of both CB and DEG source areas. The most recent sediments represented by the top layers (0–1.5 and 1.5–3 cm) suffered a sharp increase in the silt fraction, which aligns with the latter sediments transported during the event with a predominance of AG and BAN contribution, indicated by the decrease in magnetic susceptibility values together with the presence of debris leaf deposits as visible in the core image (Fig. 5). Regarding C2, similar results were obtained from both likely storm events recorded according to the magnetic susceptibility and particle size values (Fig. 6). However, in C2, AG predominates in the first and likely more intense rainfall event (7.5–17.5) with a predominance of BAN in the second and most recent event (0–7.5 cm). Both events show a higher contribution from AG and BAN at the beginning or the end of the

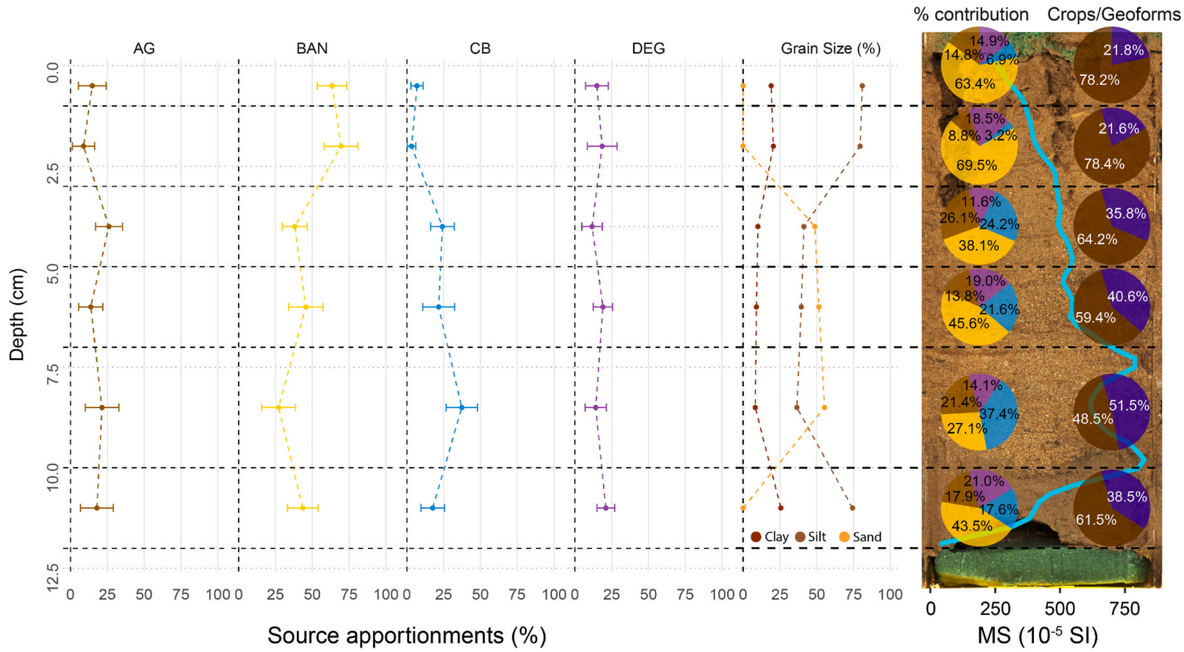

Fig. 5. Results of the unmixing procedure for the six mixture samples from core-1 (C1-1 to C1-6, 0–12 cm) for the four potential sources: agricultural (AG), banana plantation (BAN), channel bank (CB), and degraded areas (DEG). Left to right: i) mean and standard deviation (SD) contribution of each individual source to the mixtures; ii) pie charts depicting the mean percentage apportions from each sediment source to the sediment mixtures; iii) pie charts illustrating the mean percentage apportions from croplands in brown (AG + BAN) and geomorphological features in purple (CB + DEG). The cyan line on the core image represents the magnetic susceptibility values.

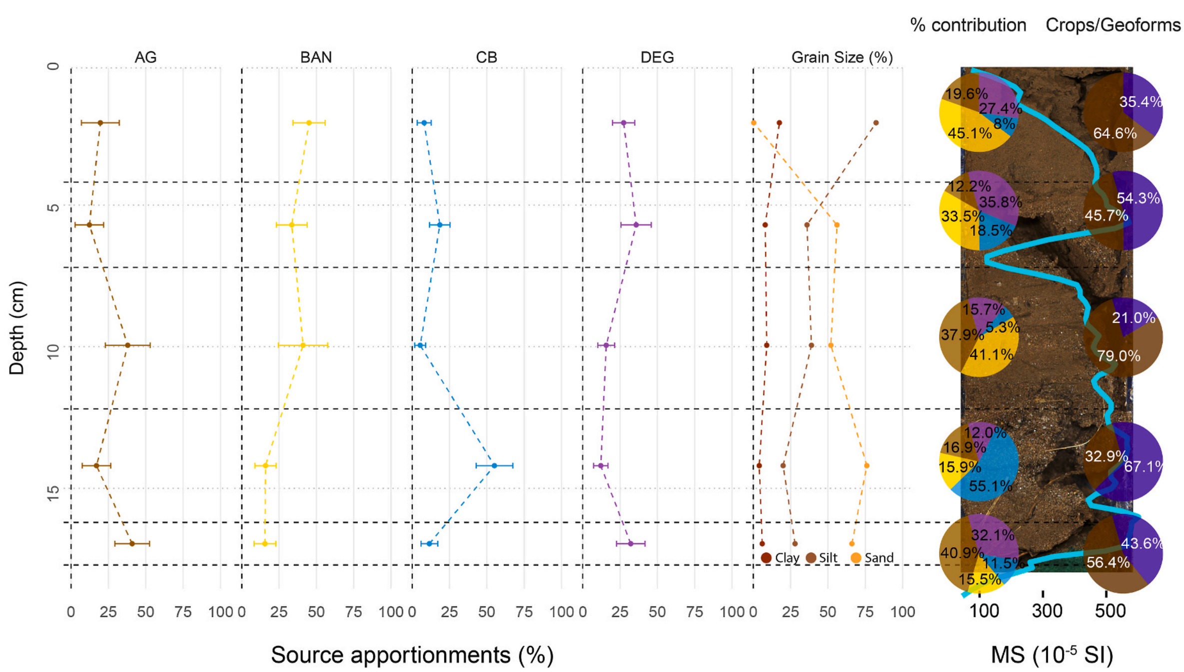

Fig. 6. Results of the unmixing procedure for the 5 mixture samples of core-2 (C2-1 to C2-5, 0–17.7 cm) for the four potential sources: agricultural (AG), banana plantation (BAN), channel bank (CB), and degraded areas (DEG). Left to right: i) mean and standard deviation (SD) contribution of each individual source to the mixtures; ii) pie charts depicting the mean percentage apportions from each sediment source to the sediment mixtures; iii) pie charts illustrating the mean percentage apportions from croplands in brown (AG + BAN) and geomorphological features in purple (CB + DEG). The cyan line on the core image represents the magnetic susceptibility values.

storm event, while the highest contribution from CB and DEG areas occurred during the high-intensity part of the storm, as concluded by the coarser grain size and magnetic susceptibility values.

4. Discussion

4.1. The spatio-temporal variability in sediment exports

The combined evidence from fluvial terrace and gravity core sediment records provided insights into the complex sediment dynamics of these tropical agricultural mountainous catchments.

The high contribution from geomorphological features such as channel bank (CB) and degraded areas (DEG) during high discharge event (T5 to T3) to the terrace sediment column is expected due to their proximity to the streams and the coarser nature of these sources. In the event-scale time sequences observed, these inputs were followed by a gradual transition to higher AG and BAN contributions as the flow intensity decreased, with a predominance of CB at low discharge intensities (T0). These results are expected because in the most active part of the channel, fine sediments are constantly washed away, and there is insufficient discharge energy to transport significant quantities of material from croplands upstream or produce runoff in banana plantations or mobilise degraded sources with predominantly coarser sediment. Additionally, the predominance of CB at low discharges could be associated with two different processes. First, high channel bank erosion during high discharge scenarios (T5 and T4) leaves unstable and fragile taluses that continually fall into the stream as easily erodible sediment for low discharge flows. Second, the finer-grained sediments from other sources have likely been transported downstream due to the river's constant flow.

During low discharges (T0), BAN sediment transport is not activated, barely reaching the stream and transporting only the loose sediment left in the main stream after the runoff event. On the other hand, T1 represents a higher discharge than T0 associated with rainfall that can produce overland flow and rill erosion, allowing mobilised sediment from the banana plantation areas to reach and accumulate in the stream. One characteristic of the banana source is the predominance of fine sediment because of its location in the lower part of the catchment. Thus, T1 represents enough energy to mobilise the BAN source sediments into the streams but not enough to transport all BAN sediments downstream, assuming a lack of soil aggerate stability due to land management practice. The agriculture contribution (AG) experiences similar patterns to the BAN source. However, as most croplands are located in the upper part of the catchment, a higher contribution is expected during higher discharges, as reflected in T1, T2, T3, and T4, while probably being less important during very high discharges (T5) due to the high contribution of degraded areas (DEG) and the rest of the sources.

Notably, the coarser fraction predominant in channel banks and degraded areas tended to accumulate in the stream due to the higher energy required for its continued transportation, while finer sediments exported from banana plantations (BAN) and crops (AG) are more easily transported downstream, ultimately reaching the lake. This is evidenced by their predominant contributions and the dominance of finer particles in the sediment cores. Residence time of this material, and entrapped fine sediment, has important implications for system recovery following rehabilitation.

While channel banks are natural sources present throughout the catchment, the contribution from degraded areas is likely primarily linked to sediment mounds accumulated by farmers on stream levees, which are then exported during storm events when water levels rise as observed during fieldworks and visible in Fig. 1f and Fig. S2. The DEG source encompasses samples from landslide scars and mining activities. However, our findings and field observations indicate that fine sediments are the predominant fraction reaching streams and being exported to the lake, suggesting that areas dominated by coarse particles, such as the DEG source, are unlikely significant contributors unless located near the streams. It is worth mentioning that these areas could contribute to specific peaks of fine sediments during events such as mass movements potentially resulting in natural hazard disasters or rock mining areas at the beginning of extraction when the topsoil is removed (Depicker et al., 2021). Although the sediment cores predominantly showed contribution from AG and BAN, during peak flow the channel bank (CB) was the main contributor. This is supported by an increase in the sand fraction and magnetic susceptibility values (Figs. 5 and 6). The finer particles from agricultural (AG) and banana (BAN) sources are likely deposited further into the lake during these high-intensity flows.

Despite the overall successful unmixing in statistical terms, implementing the CTS method allowed us to detect the presence of multiple solutions in some of the target samples that suggested the possibility of interchange between the contribution of AG and BAN sources depending on the selected tracers, especially in C2 (Table S2), i.e. the model struggled to differentiate these sources in overdetermined stable elements dataset. Therefore, field observations and additional information such as grain size and independent tracers such as magnetic susceptibility are essential for a full understanding of unmixing results that could be further augmented by triangulation with local environmental knowledge (Blake et al., 2018; Kelly et al., 2020). This challenge is not unique to the present study but is inherent in all fingerprinting studies with overdetermined systems, which result in the presence of multiple solutions (Latorre et al., 2021). Future studies should target a combined approach using tracers that better discriminate between organic sources such as seasonal crops (AG) and banana plantations (BAN) to enhance the precision of results. An ideal approach would involve integrating elemental composition data such as the one in this study with CSSI-FA tracers, as demonstrated in previous studies, to improve discrimination and ensure the availability of conservative and consensus-driven tracers (Lizaga et al., 2024). These more technical approaches combined with social science evidence could expand our insights and inform more effective strategies for addressing human-induced environmental challenges.

4.2. Land management challenges and banana disease impacts

Since the 1960s, negative human impact on the landscape has intensified due to population pressure and limited implementation of sustainable land management practices. This situation has been reinforced by armed conflicts since the 1990s leading to deforestation and survival-driven agricultural practices in the region (Büscher and Mathys, 2019). Despite the inherent quality of volcanic soils, their high erodibility combined with the lack of buffer structures and unsustainable practices like removing grass cover in banana fields contribute significantly to overland flow, erosion and runoff causing further downstream incision in low order streams. This results in substantial sediment export, nutrient depletion, and soil degradation, especially in the highlands where shallow and fragile soils predominate.

Contrary to expectations, given their dense vegetation cover, banana plantations emerge as one of the primary sources contributing fine sediment to the lake. This aligns not only with field observations but also with the fact that, despite being largely located in the lowlands and protecting the soil from direct raindrop erosion, they serve as temporary deposition areas for material mobilised from cropland located on steep slopes. Consequently, fine loose/disaggregated sediment predominates in these areas. This is exacerbated by the region's history of unsustainable agricultural practices and the complete removal of banana crops in 2010 due to banana wilt disease (BXW) (Fig. S3). Moreover, all accumulated runoff passes through banana plantations, which, combined with their proximity to streams, makes banana plantations one of the primary contributors of fine sediments to the streams.

Overall, this study provides novel insights into the complex interactions between banana plantations and sediment dynamics, particularly highlighting their unexpected role as major contributors of fine sediment to Lake Kivu. While previous studies have identified general land management issues, our research specifically quantifies the contribution of different land uses during high-intensity rainfall events. This is of global relevance given widespread predictions of future climates of extreme. Furthermore, our findings also open new research pathways for investigating additional anthropogenic impacts in the region to deepen understanding of complex non-linear feedbacks in disturbed and polluted systems. For instance, river mining activities could significantly influence sediment dynamics through major channel changes potentially producing signatures similar to those we identified from degraded areas such as landslide scars, near stone extraction activities, or mounds of sediments extracted from the stream channel beds. Understanding these combined effects is crucial for developing effective soil conservation strategies in this vulnerable region.

5. Conclusions

This research underscores the significant influence of agricultural practices and high-intensity storm events on driving the spatiotemporal variability of sediment export. Notably, the dredging of the river and the deposition of extracted sediments in mounds are identified as activities facilitating downstream sediment transport by remobilising the channel bed and leaving non-cohesive, erodible sediment readily available near streams.

Despite banana plantations offering protection against raindrop erosion and being situated at the valley bottoms, poor management practices, overland flow resulting from the absence of natural vegetation or terrace buffers uphill, and their proximity to the main channel contribute significantly to sediment export. This heightened contribution may be linked to the plantations' history, nearly eradicated due to banana wilt disease a decade before, leading to soil structure degradation and increased erodibility. The location of the seasonal crops on the upper catchment steep slopes led to a high contribution of AG source during storm events but also an increase in runoff due to the lack of forest cover or buffer structures. This increased runoff exacerbates the erosion power of these high storm events, posing a danger to downstream infrastructure. The nutrient-enriched finer fraction characteristic of croplands and banana plantations emerges as the primary sediment source exported to the lake, with channel banks and degraded sediments predominantly reaching the lake during high-intensity events with longer residence time in the streams.

The spatial-temporal design of mixture sampling, incorporating different altitude fluvial terraces and sediment cores, allows for an understanding of the hysteresis cycle of exported sediment during high-intensity storm events. This tracer-based finding highlights a negative feedback loop, with high export rates of fertile topsoils and subsequent nutrients posing risks not only to crop production but also to lake pollution, endangering fauna and fish populations.

CRediT authorship contribution statement

Ivan Lizaga: Writing – review & editing, Writing – original draft, Validation, Software, Resources, Project administration, Methodology, Investigation, Funding acquisition, Formal analysis, Data curation, Conceptualization. **Montfort Bagalwa:** Writing – review & editing, Formal analysis, Data curation. **Borja Latorre:** Writing – review & editing, Software, Investigation, Data curation. **Kristof Van Oost:** Writing – review & editing. **Ana Navas:** Writing – review & editing, Resources. **William Blake:** Writing – review & editing, Resources, Methodology. **Pascal Boeckx:** Writing – review & editing, Supervision, Resources, Methodology, Conceptualization.

Declaration of competing interest

The authors declare that they have no known competing financial interests or personal relationships that could have appeared to influence the work reported in this paper.

Acknowledgements

This study was supported by the Research Foundation-Flanders (FWO, mandate 12V8622N).

Appendix A. Supplementary data

Supplementary data to this article can be found online at https://doi.org/10.1016/j.jenvman.2024.123573.

Data availability

Data will be made available on request.

References

Bagalwa, R.M., Chartin, C., Baumgartner, S., Mercier, S., Syauswa, M., Samba, V.C., Zabona, M.T., Karume, K., Cizungu, N.L., Barthel, M., Doetterl, S., Six, J., Boeckx, P., Van Oost, K., 2021. Spatial and seasonal patterns of rainfall erosivity in the Lake Kivu region: insights from a meteorological observatory network. Prog. Phys. Geogr. Earth Environ. 45, 866–884. https://doi.org/10.1177/03091333211001793.

Baumgartner, S., Bauters, M., Barthel, M., Alebadwa, S., Bahizire, N., Sumaili, C., Ngoy, D., Kongolo, M., Bazirake, B.M., Ntaboba, L.C., Six, J., Boeckx, P., Van Oost, K., Drake, T.W., 2022. Fluvial sediment export from pristine forested headwater catchments in the Congo Basin. Geomorphology 398, 108046. https://doi.org/10.1016/j.geomorph.2021.108046.

Blake, W.H., Ficken, K.J., Taylor, P., Russell, M.A., Walling, D.E., 2012. Tracing crop-specific sediment sources in agricultural catchments. Geomorphology 139–140, 322–329. https://doi.org/10.1016/j.geomorph.2011.10.036.

Blake, W.H., Rabinovich, A., Wynants, M., Kelly, C., Nasseri, M., Ngondya, I., Patrick, A., Mtei, K., Munishi, L., Boeckx, P., Navas, A., Smith, H.G., Gilvear, D., Wilson, G., Roberts, N., Ndakidemi, P., 2018. Soil erosion in East Africa : an interdisciplinary approach to realising pastoral land management change. Environ. Res. Lett. 13.

Buchhorn, M., Smets, B., Bertels, L., Lesiv, M., Tsendbazar, N.-E., Masiliunas, D., Linlin, L., Herold, M., Fritz, S., 2020. Copernicus Global Land Service: Land Cover 100m: Collection 3: Epoch 2021. Globe. https://doi.org/10.5281/zenodo.3939050, Version V3.0.1.

Büscher, K., Mathys, G., 2019. War, displacement and rural–urban transformation: kivu's boomtowns, eastern D.R. Congo. Eur. J. Dev. Res. 31, 53–71. https://doi.org/10.1057/s41287-018-0181-0.

Clarke, R.T., 2014. A bootstrap calculation of confidence regions for proportions of sediment contributed by different source areas in a 'fingerprinting' model. Hydrol. Process. 29, 2694–2703. https://doi.org/10.1002/hyp.10397.

Collins, A.L., Pulley, S., Foster, I.D.L., Gellis, A., Porto, P., Horowitz, A.J., 2017. Sediment source fingerprinting as an aid to catchment management: a review of the current state of knowledge and a methodological decision-tree for end-users. J. Environ. Manage., Sediment source fingerprinting for informing catchment management: methodological approaches, problems and uncertainty 194, 86–108. https://doi.org/10.1016/j.jenvman.2016.09.075.

Cooper, R.J., Krueger, T., 2017. An extended Bayesian sediment fingerprinting mixing model for the full Bayes treatment of geochemical uncertainties. Hydrol. Process. 31, 1900–1912. https://doi.org/10.1002/hyp.11154.

Depicker, A., Jacobs, L., Mboga, N., Smets, B., Van Rompaey, A., Lennert, M., Wolff, E., Kervyn, F., Michellier, C., Dewitte, O., Govers, G., 2021. Historical dynamics of landslide risk from population and forest-cover changes in the Kivu Rift. Nat. Sustain. 4, 965–974. https://doi.org/10.1038/s41893-021-00757-9.

Dewitte, O., Jones, A., Spaargaren, O., Breuning-Madsen, H., Brossard, M., Dampha, A., Deckers, J., Gallali, T., Hallett, S., Jones, R., Kilasara, M., Le Roux, P., Michéli, E., Montanarella, L., Thiombiano, L., Van Ranst, E., Yemefack, M., Zougmore, R., 2013. Harmonisation of the soil map of Africa at the continental scale. Geoderma 211–212, 138–153. https://doi.org/10.1016/j.geoderma.2013.07.007.

Evrard, O., Poulenard, J., Némery, J., Ayrault, S., Gratiot, N., Duvert, C., Prat, C., Lefèvre, I., Bonté, P., Esteves, M., 2013. Tracing sediment sources in a tropical highland catchment of central Mexico by using conventional and alternative fingerprinting methods. Hydrol. Process. 27, 911–922. https://doi.org/10.1002/hyp.9421.

Gaspar, L., Lizaga, I., Blake, W.H., Latorre, B., Quijano, L., Navas, A., 2019. Fingerprinting changes in source contribution for evaluating soil response during an exceptional rainfall in Spanish pre-pyrenees. J. Environ. Manage. 240, 136–148. https://doi.org/10.1016/j.jenvman.2019.03.109.

Gruszowski, K.E., Foster, I.D.L., Lees, J.A., Charlesworth, S.M., 2003. Sediment sources and transport pathways in a rural catchment, Herefordshire, UK. Hydrol. Process. 17, 2665–2681. https://doi.org/10.1002/hyp.1296.

Huffman, G.J., Stocker, E.F., Bolvin, D.T., Nelkin, E.J., Jackson, Tan, 2019. GPM IMERG Final Precipitation L3 Half Hourly 0.1 degree x 0.1 degree V06, Greenbelt, MD. In: Goddard Earth Sciences Data and Information Services Center (GES DISC). https://doi.org/10.5067/GPM/IMERG/3B-HH/07. Accessed: [Data Access Date].

Haddadchi, A., Ryder, D.S., Evrard, O., Olley, J., 2013. Sediment fingerprinting in fluvial systems: review of tracers, sediment sources and mixing models. Int. J. Sediment Res. 28, 560–578. https://doi.org/10.1016/S1001-6279(14)60013-5.

Kelly, C., Wynants, M., Munishi, L.K., Nasseri, M., Patrick, A., Mtei, K.M., Mkilema, F., Rabinovich, A., Gilvear, D., Wilson, G., Blake, W., Ndakidemi, P.A., 2020. 'Mind the gap': reconnecting local actions and multi-level policies to bridge the governance gap. An Example of Soil Erosion Action from East Africa. Land 9, 352. https://doi.org/10.3390/land9100352.

Lizaga, I., Latorre, B., Gaspar, L., Navas, A., 2018. fingerPro V2.0: an R package for sediment source tracing. https://doi.org/10.5281/zenodo.1402029.

Lizaga, I., Gaspar, L., Blake, W.H., Latorre, B., Navas, A., 2019. Fingerprinting changes of source apportionments from mixed land uses in stream sediments before and after an exceptional rainstorm event. Geomorphology 341, 216–229. https://doi.org/10.1016/j.geomorph.2019.05.015.

Lizaga, I., Latorre, B., Gaspar, L., Navas, A., 2020a. Consensus ranking as a method to identify non-conservative and dissenting tracers in fingerprinting studies. Sci. Total Environ. 720, 137537. https://doi.org/10.1016/j.scitotenv.2020.137537.

Lizaga, I., Latorre, B., Gaspar, L., Navas, A., 2020b. FingerPro: an R Package for tracking the provenance of sediment. Water Resour. Manag. 34, 3879–3894. https://doi.org/10.1007/s11269-020-02650-0.

Latorre, B., Lizaga, I., Gaspar, L., Navas, A., 2021. A novel method for analysing consistency and unravelling multiple solutions in sediment fingerprinting. Sci. Total Environ. 789, 147804. https://doi.org/10.1016/j.scitotenv.2021.147804.

Lizaga, I., Latorre, B., Bodé, S., Gaspar, L., Boeckx, P., Navas, A., 2024. Combining isotopic and elemental tracers for enhanced sediment source partitioning in complex catchments. J. Hydrol. 631, 130768. https://doi.org/10.1016/j.jhydrol.2024.130768.

Lutete Landu, E., Ilombe Mawe, G., Makanzu Imwangana, F., Bielders, C., Dewitte, O., Poesen, J., Hubert, A., Vanmaercke, M., 2023. Effectiveness of measures aiming to stabilize urban gullies in tropical cities: results from field surveys across D.R. Congo. International Soil and Water Conservation Research 11, 14–29. https://doi.org/10.1016/j.iswcr.2022.10.003.

Martínez-Carreras, N., Krein, A., Udelhoven, T., Gallart, F., Iffly, J.F., Hoffmann, L., Pfister, L., Walling, D.E., 2010. A rapid spectral-reflectance-based fingerprinting approach for documenting suspended sediment sources during storm runoff events. J. Soils Sediments 10, 400–413. https://doi.org/10.1007/s11368-009-0162-1.

Maystadt, J.-F., Mueller, V., Hoek, J.V.D., Weezel, S. van, 2020. Vegetation changes attributable to refugees in Africa coincide with agricultural deforestation. Environ. Res. Lett. 15, 044008. https://doi.org/10.1088/1748-9326/ab6d7c.

Monsieurs, E., Kirschbaum, D.B., Tan, J., Mateso, J.-C.M., Jacobs, L., Plisnier, P.-D., Thiery, W., Umutoni, A., Musoni, D., Bibentyo, T.M., Ganza, G.B., Mawe, G.I., Bagalwa, L., Kankurize, C., Michellier, C., Stanley, T., Kervyn, F., Kervyn, M., Demoulin, A., Dewitte, O.. Evaluating TMPA Rainfall over the Sparsely Gauged East African Rift. https://doi.org/10.1175/JHM-D-18-0103.1.

Nahimana, L., 2015. Les dispositifs géologiques et les sols. Atlas des pays du Nord-Tanganyika, pp. 32–38. Planches 4a et 4b, IRD Editions, Marseille 2015.

Navas, A., Valero Garcés, B., Machín, J., 2004. Research Note: an approach to integrated assessement of reservoir siltation: the Joaquín Costa reservoir as a case study. Hydrol. Earth Syst. Sci. 8, 1193–1199. https://doi.org/10.5194/hess-8-1193-2004.

Ndayirukiye, S., Sabushimike, J.M., 2015. Les climats et les mécanismes climatiques. Atlas des pays du Nord-Tanganyika, Planche 3, 28–31. Marseille, IRD Editions,144.

Ocimati, W., Groot, J.J.C., Tittonell, P., Taulya, G., Ntamwira, J., Amato, S., Blomme, G., 2020. Xanthomonas wilt of banana drives changes in land-use and ecosystem services across infected landscapes. Sustainability 12, 3178. https://doi.org/10.3390/su12083178.

Owens, P.N., Blake, W.H., Gaspar, L., Gateuille, D., Koiter, A.J., Lobb, D.A., Petticrew, E. L., Reiffarth, D.G., Smith, H.G., Woodward, J.C., 2016. Fingerprinting and tracing the sources of soils and sediments: earth and ocean science, geoarchaeological, forensic, and human health applications. Earth Sci. Rev. 162, 1–23. https://doi.org/10.1016/j.earscirev.2016.08.012.

Palazón, L., Gaspar, L., Latorre, B., Blake, W.H., Navas, A., 2015. Identifying sediment sources by applying a fingerprinting mixing model in a Pyrenean drainage catchment. J. Soils Sediments 15, 2067–2085. https://doi.org/10.1007/s11368-015-1175-6.

Pérez, I.J., Cabrerizo, F.J., Alonso, S., Dong, Y.C., Chiclana, F., Herrera-Viedma, E., 2018. On dynamic consensus processes in group decision making problems. Inf. Sci. 459, 20–35. https://doi.org/10.1016/j.ins.2018.05.017.

Pulley, S., Foster, I., Antunes, P., 2015. The uncertainties associated with sediment fingerprinting suspended and recently deposited fluvial sediment in the Nene river basin. Geomorphology 228, 303–319. https://doi.org/10.1016/j.geomorph.2014.09.016.

Smith, H.G., Blake, W.H., 2014. Sediment fingerprinting in agricultural catchments: a critical re-examination of source discrimination and data corrections. Geomorphology 204, 177–191. https://doi.org/10.1016/j.geomorph.2013.08.003.

Vanmaercke, M., Poesen, J., Van Mele, B., Demuzere, M., Bruynseels, A., Golosov, V., Bezerra, J.F.R., Bolysov, S., Dvinskih, A., Frankl, A., Fuseina, Y., Guerra, A.J.T., Haregeweyn, N., Ionita, I., Makanzu Imwangana, F., Moeyersons, J., Moshe, I., Nazari Samani, A., Niacsu, L., Nyssen, J., Otsuki, Y., Radoane, M., Rysin, I., Ryzhov, Y.V., Yermolaev, O., 2016. How fast do gully headcuts retreat? Earth Sci. Rev. 154, 336–355. https://doi.org/10.1016/j.earscirev.2016.01.009.

Walling, D.E., 2005. Tracing suspended sediment sources in catchments and river systems. Sci. Total Environ. 344, 159–184. https://doi.org/10.1016/j.scitotenv.2005.02.011.

Winston, W.E., Criss, R.E., 2002. Geochemical variations during flash flooding, Meramec River basin, May 2000. J. Hydrol. 265, 149–163. https://doi.org/10.1016/S0022-1694(02)00105-1.

Zanaga, D., Van De Kerchove, R., Daems, D., De Keersmaecker, W., Brockmann, C., Kirches, G., Wevers, J., Cartus, O., Santoro, M., Fritz, S., Lesiv, M., Herold, M., Tsendbazar, N.E., Xu, P., Ramoino, F., Arino, O., 2022. ESA WorldCover 10 m 2022 v200. https://doi.org/10.5281/zenodo.7254221.

Zhang, J., Yang, M., Zhang, F., Zhang, W., Zhao, T., Li, Y., 2017. Fingerprinting sediment sources after an extreme rainstorm event in a small catchment on the loess plateau, PR China. Land Degrad. Dev. 28, 2527–2539. https://doi.org/10.1002/ldr.2803.